

Hydration and Physico-mechanical Properties of Blended Calcium Sulfoaluminate-belite Cement Made of Industrial By-products

Atchara Rungchet

Department of Physics and Materials Science, Faculty of Science, Chiang Mai University, Chiang Mai, Thailand

Prinya Chindapasirt

Sustainable Infrastructure Research and Development Center, Department of Civil Engineering, Faculty of Engineer, Khon Kaen University, Khon Kaen, Thailand

Chi-Sun Poon

Department of Civil and Environmental Engineering, The Hong Kong Polytechnic University, Hong Kong

Kedsarin Pimraksa*

Department of Industrial Chemistry, Faculty of Science, Chiang Mai University, Chiang Mai, Thailand

* Corresponding author. E-mail: kedsarin.p@cmu.ac.th DOI: 10.14416/j.ijast.2016.11.006

Received: 25 August 2016; Accepted: 13 September 2016; Published online: 17 November 2016

© 2016 King Mongkut's University of Technology North Bangkok. All Rights Reserved.

Abstract

Portland cement blended Calcium Sulfoaluminate-belite (C \hat{S} AB) cements were studied in order to improve its binding properties and workability for specific applications. The binders consisted of calcium sulfoaluminate-belite, Flue Gas Desulfurization-gypsum and Ordinary Portland Cement (OPC). In this research, effects of OPC contents (25, 50, 75 wt%) as a C \hat{S} AB replacement on hydration behaviors and physico-mechanical properties of the binders were observed. Used C \hat{S} AB cement was synthesized using industrial by-products viz., fly ash, Flue Gas Desulfurization-gypsum, Al-rich sludge as starting materials via hydrothermal-calcination method. The results revealed that the replacement of C \hat{S} AB cement with OPC extended the setting times of pastes. The reduction of hydration rate with higher OPC content was due to dilution of fast setting phases such calcium sulfoaluminate and mayenite. Hydration products of calcium sulfoaluminate cement were ettringite responsible for high early strength together with Al(OH)₃. From 6 h onwards, hydration of tricalcium silicate phase from the OPC generated calcium silicate hydrate. Strätlingite was also found in low OPC content mix resulting from the reaction between the Al(OH)₃ and either alite phase in OPC or belite phase in C \hat{S} AB cement. Ettringite could also react with Al(OH)₃ to generate monosulfate at later ages. The calcium sulfoaluminate phase was mainly responsible for the early mechanical properties, while OPC played an important role to improve strength at later ages.

Keywords: Blended cement, Calcium Sulfoaluminate-belite cement, Ordinary Portland Cement, Flue Gas Desulfurization-gypsum, Hydration

Please cite this article as: A. Rungchet, P. Chindapasirt, C. S. Poon, and K. Pimraksa, "Hydration and physico-mechanical properties of blended calcium sulfoaluminate-belite cement made of industrial by-products," *KMUTNB Int J Appl Sci Technol*, vol. 9, no. 4, pp. 279–287, Oct.–Dec. 2016.

1 Introduction

Calcium Sulfoaluminate-belite (C \hat{S} AB) cements are recently received highly attention as an alternative binder to Ordinary Portland Cement (OPC). This is not only due to their low lime content, low calcination temperature (1250°C) and the improved grindability, but also the possibility of using a large amount of industrial wastes materials, such as fly ash, red mud and FGD-gypsum as raw materials [1], [2]. The basic components of C \hat{S} AB cement are calcium sulfoaluminate (4CaO.3Al₂O₃.SO₃; C₄A₃ \hat{S}), dicalcium silicate (2CaO.SiO₂; C₂S), tetra calcium aluminoferrite (4CaO.Al₂O₃.Fe₂O₃; C₄AF) and calcium sulfate (CaO.SO₃; C \hat{S}) with some aluminate phases as a minority. The amount of each phases depends on the composition and proportions of the raw materials used for clinkerization [3], [4].

C \hat{S} AB cements show a rapid hardening and provides high early-age strength because of the rapid formation of ettringite (C₃A.3C \hat{S} .32H; C₆A \hat{S} ₃H₃₂) and aluminum hydroxide (Al(OH)₃; AH₃) [5]–[7], which arise from the hydration reaction between C₄A₃ \hat{S} and calcium sulfate compound. Calcium sulfate compound can be either in a form of anhydrite (CaSO₄; C \hat{S}) in the synthesized cement or gypsum (CaSO₄.2H₂O; C \hat{S} H₂) or the combination of the two phases, co-ground with clinker after calcination. The long-term strength of C \hat{S} AB cement is contributed from the hydration of C₂S [8], which generates calcium silicate hydrate (C–S–H) and calcium aluminosilicate hydrate (CASH) in a form of strätlingite, and calcium hydroxide (Ca(OH)₂; CH). This reaction is much slower than that of C₄A₃ \hat{S} .

Previous study of the authors [9] has shown a successful production of C \hat{S} AB cement from fly ash and other industrial wastes (FGD-gypsum and Al-rich sludge) using hydrothermal-calcination method. The hydrothermal-calcination developed by Jiang & Roy has been accepted to be energy saving pathway for belite cement synthesis [10]. During its production, this kind of cement releases less CO₂ than OPC clinker for essential two reasons: the calcination temperature is only 1050°C (1450°C for Portland cement) and the lime content is lower. For the conditions employed in previous work [9], C \hat{S} AB cements and gypsum could achieve fast setting and rapid hardening because of its large surface area associated with highly reactive phase such as mayenite phase (Ca₁₂Al₁₄O₃₃; C₁₂A₇).

This could hinder the workability of cement slurry.

Portland cement is a hydraulic binder, obtained from a clinkerization process of limestone, sand, clay and iron ore. OPC mainly composed of five phases, tricalcium silicate (3CaO.SiO₂; C₃S), dicalcium silicate (2CaO.SiO₂; C₂S), tricalcium aluminate (3CaO.Al₂O₃; C₃A), calcium aluminoferrite (4CaO.Al₂O₃.Fe₂O₃; C₄AF) and calcium sulfate dihydrate (CaSO₄.2H₂O; C \hat{S} H₂) [11]. After hydration, OPC exhibits good flow ability (flow value of 110 ± 5 at normal consistency), slow setting and high later-age strength [12], [13]. These promising properties cannot be reached using C \hat{S} AB-based cement paste alone. For these reasons, binary binders (OPC–C \hat{S} AB cement) is considered an interesting alternative for the improvement of C \hat{S} AB workability and properties.

Portland cement blended calcium sulfoaluminate-belite cements are therefore considered to lever the difficulty in workability as well as to improve the mechanical properties. Concrete made using binary and ternary binders can provide desirable properties for particular purposes, such as reduction of total heat evolution in massive structures, improvement of durability and early strength modification above the normal range [14], [15].

This research aimed to study the hydration behaviors and physico-mechanical properties of the Portland cement blended C \hat{S} AB cement. The replacement levels of C \hat{S} AB cement with OPC as 25, 50 and 75 wt% were investigated in order to improve compressive strength and to formulate slow setting/hardening of binder system for specific applications.

2 Experimental Procedure

2.1 Raw materials preparation

Portland cement Type I (OPC), Synthesized C \hat{S} AB cement and FGD-gypsum (FGDG) were used as the starting materials. The FGDG was required for the hydration of calcium sulfoaluminate phase which contained in C \hat{S} AB cement. The median particle sizes (d_{50}) of OPC, C \hat{S} AB cement and FGDG are 16, 17 and 44 μm, respectively.

The synthesized C \hat{S} AB cements were synthesized via hydrothermal-calcination method using a combination of industrial wastes viz., fly ash (FA) and FGD-gypsum (FGDG) from Mae Moh power plant in the north of

Table 1: Chemical compositions of the used materials

Raw Materials	Chemical Compositions (wt%)										
	SiO ₂	Al ₂ O ₃	Fe ₂ O ₃	CaO	Na ₂ O	K ₂ O	MgO	MnO	TiO ₂	SO ₃	LOI
OPC	21.75	5.32	3.28	64.42	-	-	1.02	0.16	0.30	3.75	n/a
CŜAB	4.21	19.10	5.05	53.23	<0.01	<0.01	0.61	0.04	0.20	17.56	n/a
FGDG	1.26	0.12	0.39	47.81	-	-	-	-	-	50.42	n/a

Thailand, and Al-rich sludge (AS) from aluminum anodizing or powder coating industrial process of Zodiac Aircatering Equipment (Thailand) Ltd., and commercial grade hydrated lime (Ca(OH)₂; CH). FA, FGDG, AS and CH were used as a source of SiO₂ and Al₂O₃, SO₃, Al₂O₃ and SO₃ and CaO, respectively. The proportion of raw ingredients was 45% CH, 20% FA, 25% AS and 10% FGDG by weight. The raw mixes were dispersed in deionized water with a liquid to solid ratio of 7 by stirring at 250 rpm for 1 h. The suspension was subjected to hydrothermal condition under atmospheric pressure (1 bar) at 130°C for reacting times of 3 h. After hydrothermal treatment, the suspension was filtered and dried at 60°C for 24 h to remove adsorbed water. The hydrothermal product was calcined in an electric furnace at a temperature of 1050°C, with a heating rate of 5°C/min and soaked at 1050°C for 1 h. This was followed by rapid air cooling [9].

The chemical compositions of raw materials were identified by X-ray fluorescence (XRF), are shown in Table 1. The mineralogical compositions determined by the X-ray diffraction (XRD) using Rietveld refinement are given in Table 2. The synthesized CŜAB cements contained 76.2 wt% ye'elimite (C₄A₃Ŝ), 9.7 wt% β-C₂S and some of C₁₂A₇, C₄AF and CŜ as minor phases. The FGDG mainly contained calcium sulfate dihydrate together with some anhydrite (2.5 wt%).

Portland cement blended CŜAB cements were produced by combining of CŜAB cement, FGDG and OPC. CŜAB was replaced by OPC at levels of 25, 50 and 75% by mass of dry solid and with a sulfoaluminate/gypsum molar ratio of 3:1, which presented in OPC:CŜAB:FGDG mass ratios as 1.33:3:1, 4:3:1 and 12:3:1, respectively. The proportion of cement mixes and water to binder (w/b) ratios of the blended CŜAB cements are shown in Table 3. PC0, PC25, PC50, PC75 and PC100 were referred to the blended mixtures with different OPC contents as 0, 25, 50, 75 and 100%, respectively.

Table 2: Mineralogical compositions using Rietveld refinement and characteristics of CŜAB cement and FGDG

Phase	Mineralogical Composition (wt%)	
	CŜAB	FGDG
C ₄ A ₃ Ŝ	76.2	-
C ₂ S	9.7	-
C ₁₂ A ₇	6.9	-
C ₄ AF	2.6	-
CŜ	3.6	2.5
CŜH ₂	-	97.5
C	0.8	-
MgO	0.2	-
Density (g/cm ³)	2.55	2.92
Surface area (m ² /kg)	1275	380

Table 3: Proportions of cement mixes for blended CŜAB cements

Symbol	Proportion of Raw Mixes (wt%)			w/b Ratio	Flow Value (mm)
	CŜAB Cement		OPC		
	CŜAB	FGDG			
PC0	75.00	25.00	0	0.80	135 ± 2
PC25	56.25	18.75	25	0.80	
PC50	37.50	12.50	50	0.65	
PC75	18.75	6.25	75	0.45	
PC100	-	-	100	0.45	

2.2 Mixing procedures

The experiments were performed at 25°C. The water/binder ratios (w/b) were varied from 0.45 to 0.80 for cement paste preparation. Flow of cement mixture slurry was kept constant as 135±2 mm. To prepare samples, cement mixes were gradually sipped into water and mixed with 150 rpm mixer for 2 min to obtain homogenous slurries. After mixing, the mixtures were cast in 2.5×2.5×2.5 cm³ of acrylic cube mold.

The specimens were demolded in 6 h and cured in a humidity chamber at $20^{\circ}\text{C} \pm 5$ and 95% relative humidity until a day of testing.

2.3 Sample characterization and testing

2.3.1 Isothermal Conduction Calorimetry (ICC)

Heat flow of each blended cement mix after hydration was measured using isothermal heat conduction calorimeter (I-CAL 4000). 30 g of the blended cement powders were used. W/b ratios of the blended cement mixes were varied from 0.45 to 0.80 according to sample preparation as mentioned above.

2.3.2 Setting time and compressive strength test

Cement pastes were prepared with varied water to binder ratios as mentioned above. The setting time tests were performed on the blended samples by allowing a 1-mm Vicat needle to settle into the paste. The initial setting time was the time elapsed between the initial contact of cement and water and the time when the needle penetration was measured to be 25 mm. The final time of setting was the time elapsed between initial contact of cement and water and the time when the needle did not leave a complete circular impression in the paste surface.

After the specimens were cured for 6 h, 12 h, 1, 3, 7, 28 and 90 d, the compressive strengths were tested using an unconfined compression machine with a maximum load of 100 kN. The loading rate of the machine was 5 mm/min. Three specimens were used for each test and the setting times and strengths were averaged.

2.3.3 X-ray Diffraction (XRD)

In order to investigate mineralogical compositions of the samples, 10 g of each mix was prepared and stored in 25 ml polyethylene cup and kept at 20°C for 6 h, 1, 7 and 28 d. Prior to XRD, the pastes were crushed, placed in ethanol for 24 h followed by drying at 40°C for 24 h in order to stop hydration. All samples were ground to obtain particles pass sieve No. 100. The instrument was operated under 40 keV and 30 mA, the step size $0.02^{\circ}/6\text{ s}$. The powdered samples were scanned between 5° and 60° (2θ) with the X'Celerator detector.

2.3.4 Scanning Electron Microscopy (SEM)

For scanning electron microscopy (Hitachi S-3700N), hydration of samples was stopped by immersing the samples in ethanol solution for 24 h followed by drying at 40°C for 24 h before vacuum impregnation in epoxy resin. The microscope was operated at 15 kV for the acquisition of backscattered electron images and EDX semi-quantitative analyses were used to quantify the main phases. PC25 sample at 28 d of curing was chosen for elemental distribution analysis using an electron probe micro-analyzer (INCAWave 500i WDS) for the generation of the elemental maps. This method was based on the segmentation of grey levels from backscattered electron images.

3 Results and Discussion

3.1 Hydration behavior

Heat flow curves of pure C $\hat{\text{S}}$ AB, blended C $\hat{\text{S}}$ AB and pure OPC are shown in Figure 1. The heat flow curve during the initial period of hydration (0–1 h) was very immense and sharp while curve during the main hydration period (1–12 h) was smaller and broad. First and second peaks of C $\hat{\text{S}}$ AB cement (PC0) were developed very rapidly designating the development of ettringite via dissolution and precipitation from $\text{C}_4\text{A}_3\hat{\text{S}}$ and C_{12}A_7 according to Eq. (1) [6], [7] and Eq. (2) [16], respectively. For PC0 [Figure 1 (a)], the third peak of heat release occurred within only 2 h due to a further rapid dissolution of $\text{C}_4\text{A}_3\hat{\text{S}}$ after sulfates in solution have been depleted due to the initial reaction resulting in the formation of monosulfate ($\text{C}_3\text{A}\cdot\text{C}\hat{\text{S}}\cdot 12\text{H}$; $\text{C}_4\text{A}\hat{\text{S}}\text{H}_{12}$) according to Eq. (3) [17]. Heat flows of the blended C $\hat{\text{S}}$ AB mixes during 1 d showed significantly different heat release with different OPC contents from pure C $\hat{\text{S}}$ AB cement as given in Figure 1 (b). It can be seen that the heat flow decreased during the first hours with an increase in OPC contents. The heat flow curves of PC25 and PC75 showed three peaks suggesting a more complex hydration evolution of the blended system with the formation and conversion of hydration products. First peak took place very rapidly and second one had a maximum heat flow around 36 and 60 min, and the third peaks were approximately 6 and 10 h for PC25 and PC75, respectively. It should be noted that the partial replacement of C $\hat{\text{S}}$ AB cement with OPC

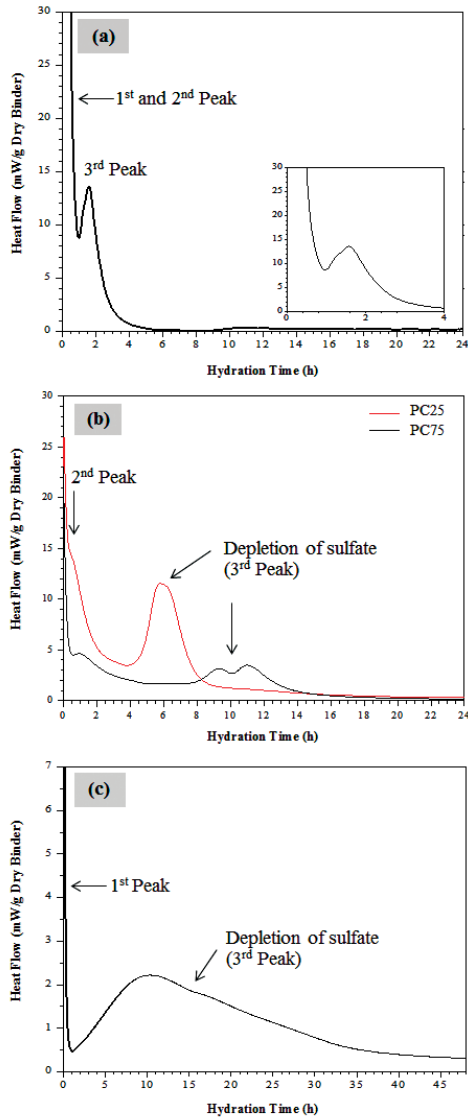
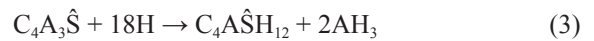
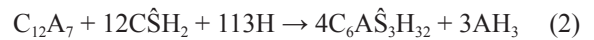
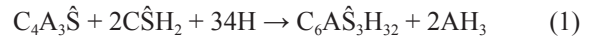


Figure 1: Heat flow curves of (a) PC0, (b) PC25 and PC75 and (c) PC100.

could delayed the hydration reaction of the blends.

For the blended cement, the third peak of heat release was obtained from hydration of OPC components such as alite (C_3S) and aluminite (C_3A), which resulted in a broad exotherm and was similar to OPC heat flow curve as given in Figure 1 (c). According to Eqs. (4) and (5), C_3S and C_3A phases were rapidly hydrated, leading to the formation of C–S–H and ettringite, respectively. The C_3S and C_3A hydration underwent in

parallel until the mixture was run out of sulfate ions in the pore solution, indicated by the sulfate depletion peak. The sulfate depletion peak relevant to the renewed hydration of C_3A occurred much later in the OPC, at around 15 h, compared to the PC75 and PC25, respectively. This was due to a decrease in sulfates ions in pore solution, which could accelerate the hydration of pastes.



3.2 Setting time and compressive strength

Table 4 presents the initial and final setting times of the blended C \hat{S} AB cements. The extendible time of binder was obtained from the presence of OPC. The initial setting values of PC0, PC25 and PC75 were 11, 22 and 65 min, respectively. The setting times of the cements were delayed as results of a reduction of early hydration phases such $C_4A_3\hat{S}$ and $C_{12}A_7$ with a replacement of OPC.

Table 4: Setting times of C \hat{S} AB, blended C \hat{S} AB and OPC cement pastes

Sample	Initial Setting Time (min)	Final Setting Time (min)
PC0 (C \hat{S} AB)	11	24
PC25	22	46
PC50	35	80
PC75	65	110
PC100 (OPC)	289	540

The variation of the OPC content provided a strong impact on the early hydration kinetics of the cement at constant $C_4A_3\hat{S}/C\hat{S}H_2$ ratio. The molar ratio of $C_4A_3\hat{S}/C\hat{S}H_2$ was 3:1 at which the C \hat{S} molar ratio was less than the requirement as stated in Eq. (1). At early hydration time (6 h–3 d), PC50 and PC75 could give higher compressive strength than PC0 and OPC as shown in Figure 2. It was mainly due to $C_4A_3\hat{S}$ hydration to form ettringite according to Eq. (1). With

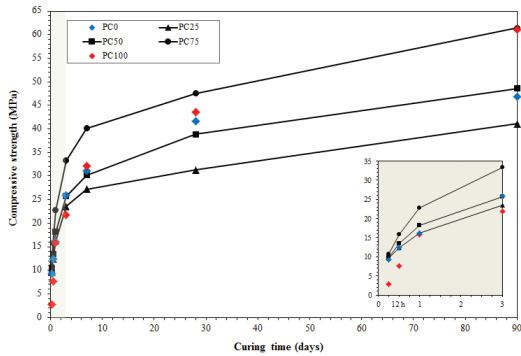


Figure 2: Compressive strength of C\$AB, blended C\$AB and OPC pastes with different curing times.

the presence of CH from OPC hydration, ettringite could be produced more massively when compared to pure C\$AB (PC0) according to Eq. (6) [18]. In addition, the high early strength of the blends was due to the presence of C₃S (OPC main component) that could give C–S–H as a hydration product after 1 d of hardening [Eq. (4)]. According to Eq. (5), the additional ettringite could be formed from the C₃A hydration. However, after 7 days of hardening, the higher OPC content (PC25 and PC50) showed lower compressive strength than PC0 and PC100 caused by a reduction of C\$AB content. An increased fraction of OPC (PC75) resulted in a higher volume of calcium silicate hydrate and thus a lower porosity and a higher compressive strength. OPC could also play a role on late hydration with 75 wt% OPC content because it contained C₂S for late hydration reactions that formed C–S–H according to Eq. (7).



Thus, the development of early strength in the binder was due to the hardening of ettringite from the hydration reaction of C₄A₃\$ with gypsum and of Portland cement components (C₃S and C₃A) while later age strength development was ascribed to the formation of C–S–H from the hydration reaction of additional C₂S from OPC blending. However, early strengths gained from PC75 sample which was cured at 1–3 days were behind when compared to Trauchessec’s finding but the later strength could be comparable [19].

This was due to the different starting cementing phases used in these experiments, such as type of calcium sulfate compound, C₄A₃\$ percentage and OPC content.

3.3 Phase composition of hydrated C\$AB-cement blends

The changes of phase compositions of PC25 and PC75 with different curing time were determined by XRD as shown in Figure 3. After 6 h of hydration, ettringite was formed together with some AH₃ from the hydration reaction of C₄A₃\$ with gypsum. The amount of ettringite in PC25 pastes was higher than PC75 with an increase in curing times due to dilution of calcium sulfoaluminate phase. C₃S was consumed at 6 h of hydration producing C–S–H in association with portlandite (Ca(OH)₂; CH) according to Eq. (4). Strätlingite started to form rapidly after 1 d as a result of the chemical reaction between the C₃S and AH₃, in agreement with [19], which could be explained using Eq. (8). C₃S involved in the strätlingite-forming reaction as shown in Figure 3 (a). The amount of AH₃ was the limiting factor for the formation of strätlingite. When OPC content was increased, in other words, a low C\$AB, resulted in a lower ettringite and AH₃ contents. This directly influenced the formation of strätlingite. Its occurrence is in blends of hydrated Portland cement with high alumina and silica. It plays a great role on strength development of high alumina cements [20].

In addition, no strätlingite was found in PC75 pastes [Figure 3 (b)]. There was a finding with the hypothesis about high stability of strätlingite with an absence of CH [20], [21]. It was also proven that with higher OPC content implying to higher Ca(OH)₂ content, strätlingite could not be formed. Ca(OH)₂ which was a byproduct of alite and belite hydration was found up to 28 d of curing time. At 7 d of curing, ettringite reacted further with AH₃ to generate monosulfate because of the depletion of gypsum according to Eq. (9). A right proportion of these hydration products (ettringite, C–S–H and strätlingite) provided the binding matrix with high compressive strength for the C\$AB blends.



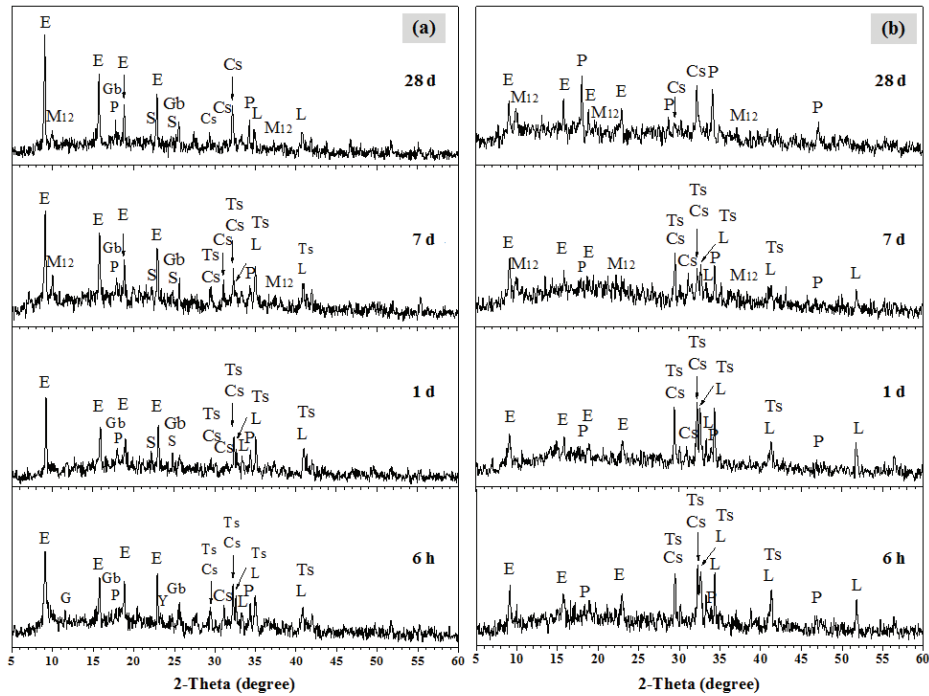


Figure 3: XRD patterns of (a) PC25 and (b) PC75 blends after 6 h, 1, 7 and 28 d of curing.

NOTE: Y: Ye'elimite ($C_4A_3\bar{S}$) G: Gypsum ($C\bar{S}H_2$) E: Ettringite ($C_6A_3\bar{S}_3H_{32}$)
 M₁₂: Monosulfate ($C_4A\bar{S}H_{12}$) P: Portlandite (CH) Ts: Tricalcium silicate (C_3S) L: Larnite (C_2S)
 Cs: Calcium silicate hydrate ($C_{1.5}SH_x$) Gb: Gibbsite (AH_3) S: Stratlingite (C_2ASH_8)

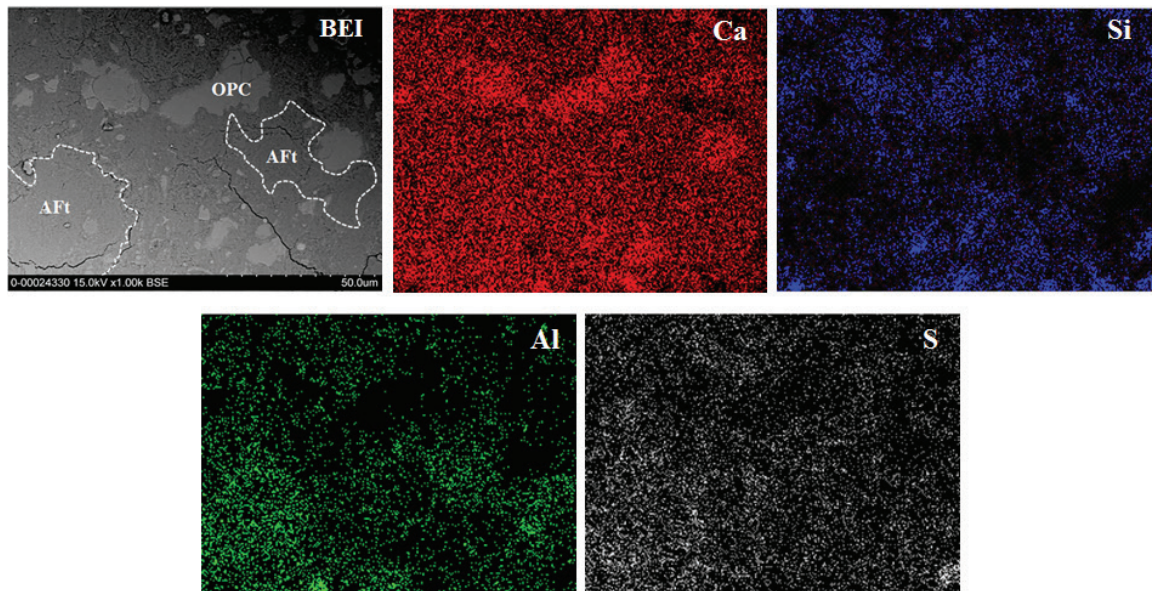


Figure 4: Backscattered electron image and WDS elemental mapping of PC25 paste at 28 d of curing.

3.4 Microstructure and elemental mapping of blended cement

Backscattered electron images clearly show phase development of PC25 at 28 d of hardening, as shown in Figure 4. From WDS elemental mappings, the presences of ettringite (Aft) and leftover C_2S phase were confirmed [14], [22]. The dark grey areas consisted of Al in high level, and Ca and S in lower level. These areas were derived from ettringite phase formation, from the hydration of $C_4A_3\hat{S}$ [14]. The lighter grey areas contained high level of Ca and lower level of Si. In these areas with C_2S phase as a reference, no Al and S were found [22]. It should be noted that in OPC blended C \hat{S} AB cement with a high proportion of C \hat{S} AB cement such a PC25, OPC hydration mainly occurred after several days and the leftover C_2S was still found at 28 d. While $C_4A_3\hat{S}$ phase was responsible for the hydration of the binder and almost fully consumed at 1 d [Figure 3 (a)], no $C_4A_3\hat{S}$ was found at 28 d of hydration.

4 Conclusions

The variation of the OPC content had strong influence on the hydrated assemblage of the binary binders. Based on this study, the following conclusions could be drawn as follows;

- With low OPC content (25 wt%), an increase in hardening speed was due to a rapid ye'elinite hydration occurring within the first 6 h that formed mainly ettringite and aluminium hydroxide. This early hydration reaction resulted in high early strength with value up to ~10 MPa measured at 6 h. After 6 h, C_3S from the OPC started to be hydrated resulting in formation of C–S–H and strätlingite, while ettringite reacted with aluminium hydroxide to generate monosulfate at later ages.
- With higher OPC contents (50 and 75 wt%), the hardening speed was lowered. OPC underwent hydration during the first days and almost fully consumed at 28 days. Ye'elinite hydration in the presence of calcium hydroxide (from OPC hydration) could provide additional ettringite. Monosulfate could be formed from the reaction between ettringite and aluminium hydroxide, indicating a lack of gypsum. No strätlingite was found in these pastes as the strätlingite was

only stable in the absence of calcium hydroxide indicating the left over calcium hydroxide and insufficient aluminium hydroxide. The high fraction of OPC resulted in a higher volume and variety of the hydrated phases and thus lower porosity and higher compressive strength. Not only strength improvement, but the blended systems also provided the better workability allowing to be practically used.

According to this laboratory experiments, the calcium sulfoaluminate phase was mainly responsible for the early mechanical properties, while ordinary Portland cement played an important role at later ages. This binder can be used in various applications depending on the desired properties. The results pointed out low OPC content (25 wt%) as the best proportion to be used in mortars for engineering applications where rapid setting (46 min) and high early strength are needed. However, if the increment of working time on the construction sites and high strength development are demanded, high OPC content (75 wt%) is the best option.

Acknowledgements

The authors gratefully acknowledge the financial supports from the Royal Golden Jubilee (RGJ) Ph.D. program and Grant No. PHD/0070/2556; Khon Kaen University and the Thailand Research Fund (TRF) under the TRF Senior Research Scholar, Grant No. RTA 5780004.

References

- [1] P. Arjunan, M. R. Silsbee, and D. M. Roy, "Sulfoaluminate-belite cement from low-calcium fly ash and sulfur-rich and other industrial by-products," *Cement and Concrete Research*, vol. 29, pp. 1305–1311, 1999.
- [2] M. Singh, S. N. Upadhayay, and P. M. Prasad, "Preparation of special cements from red mud," *Waste Management*, vol. 16, pp. 665–670, 1996.
- [3] J. H. Sharp, C. D. Lawrence, and R. Yang, "Calcium sulfoaluminate cements—low—energy cements, special cements or what?," *Advances in Cement Research*, vol. 11, pp. 3–13, 1999.
- [4] J. Majling, S. Sahu, M. Vlana, and D.M. Roy, "Relationship between raw mixture and

- mineralogical composition of sulphoaluminate belite clinkers in the system $\text{CaO-SiO}_2\text{-Al}_2\text{O}_3\text{-Fe}_2\text{O}_3\text{-SO}_3$,” *Cement and Concrete Research*, vol. 23, pp. 1351–1356, 1993.
- [5] M. García-Maté, A. G. De la Torre, L. León-Reina, E. R. Losilla, M. A. G. Aranda, and I. Santacruz, “Effect of calcium sulfate source on the hydration of calcium sulfoaluminate eco-cement,” *Cement and Concrete Composites*, vol. 55, pp. 53–61, 2015.
- [6] F. Winnefeld and S. Barlag, “Calorimetric and thermogravimetric study on the influence of calcium sulfate on the hydration of ye’elimite,” *Journal of Thermal Analysis and Calorimetry*, vol. 101, pp. 949–957, 2009.
- [7] F. Winnefeld and B. Lothenbach, “Hydration of calcium sulfoaluminate cements—Experimental findings and thermodynamic modelling,” *Cement and Concrete Research*, vol. 40, pp. 1239–1247, 2010.
- [8] H. J. H. Brouwers, “Chemical reactions in hydrated ordinary portland cement based on the work by powers and brownyard,” in *Proceedings 15th Ibausil, International Conference on Building Materials (Internationale Baustofftagung)*, Weimar, Germany, Sep. 24–27, 2003, pp. 1–0553.
- [9] A. Rungchet, P. Chindapasirt, S. Wansom, and K. Pimraksa, “Hydrothermal synthesis of calcium sulfoaluminate–belite cement from industrial waste materials,” *Journal of Cleaner Production*, vol. 115, pp. 273–283, 2016.
- [10] K. Pimraksa, S. Hanjitsuwan, and P. Chindapasirt, “Synthesis of belite cement from lignite fly ash,” *Ceramics International*, vol. 35, pp. 2415–2425, 2009.
- [11] I. Odler, *Special Inorganic Cements*, CRC Press, 2003, pp. 7–15.
- [12] *Standard Test Method for Compressive Strength of Hydraulic Cement Mortars (Using 2-in. or [50-mm] Cube Specimens)*, ASTM C109, 2013.
- [13] *Standard Specification for Portland Cement*, ASTM C150, 2012.
- [14] L. Pelletier, F. Winnefeld, and B. Lothenbach, “The ternary system Portland cement–calcium sulfoaluminate clinker–anhydrite: Hydration mechanism and mortar properties,” *Cement and Concrete Composites*, vol. 32, pp. 497–507, 2010.
- [15] C. Cau Dit Coumes, S. Courtois, S. Peysson, J. Ambroise, and J. Pera, “Calcium sulfoaluminate cement blended with OPC: A potential binder to encapsulate low-level radioactive slurries of complex chemistry,” *Cement and Concrete Research*, vol. 39, pp. 740–747, 2009.
- [16] M. C. Martín-Sedeño, A. J. M. Cuberos, Á. G. De la Torre, G. Álvarez-Pinazo, L.M. Ordóñez, M. Gateshki, and M.A.G. Aranda, “Aluminum-rich belite sulfoaluminate cements: Clinkering and early age hydration,” *Cement and Concrete Research*, vol. 40, pp. 359–369, 2010.
- [17] I. A. Chen and M. C. G. Juenger, “Synthesis and hydration of calcium sulfoaluminate-belite cements with varied phase compositions,” *Journal of Materials Science*, vol. 46, pp. 2568–2577, 2010.
- [18] C. W. Hargis, A. P. Kirchheim, P. J. M. Monteiro, and E. M. Gartner, “Early age hydration of calcium sulfoaluminate (synthetic ye’elimite, $\text{C}_4\text{A}_3\text{S}$) in the presence of gypsum and varying amounts of calcium hydroxide,” *Cement and Concrete Research*, vol. 48, pp. 105–115, 2013.
- [19] R. Trauchessec, J.-M. Mechling, A. Lecomte, A. Roux, and B. Le Rolland, “Hydration of ordinary Portland cement and calcium sulfoaluminate cement blends,” *Cement and Concrete Composites*, vol. 56, pp. 106–114, 2015.
- [20] H.G. Midgley and P. Bhaskara Rao, “Formation of strätlingite, $2\text{CaO}\cdot\text{SiO}_2\cdot\text{Al}_2\text{O}_3\cdot 8\text{H}_2\text{O}$, in relation to the hydration of high alumina cement,” *Cement and Concrete Research*, vol. 8, pp. 169–172, 1978.
- [21] M.U. Okoronkwo and F.P. Glasser, “Strätlingite: compatibility with sulfate and carbonate cement phases,” *Materials and Structures*, vol. 49, pp. 3569–3577, 2015.
- [22] I. A. Chen and M. C. G. Juenger, “Incorporation of coal combustion residuals into calcium sulfoaluminate-belite cement clinkers,” *Cement and Concrete Research*, vol. 34, pp. 893–902, 2012.